

---

# Reinforcement Learning for Diffusion LLMs with Entropy-Guided Step Selection and Stepwise Advantages

---

Vishnu Teja Kunde<sup>\*1</sup> Fatemeh Doudi<sup>\*1</sup> Mahdi Farahbakhsh<sup>1</sup> Dileep Kalathil<sup>1</sup> Krishna Narayanan<sup>1</sup>  
Jean-Francois Chamberland<sup>1</sup>

## Abstract

Reinforcement learning (RL) has been effective for post-training autoregressive (AR) language models, but extending these methods to diffusion language models (DLMs) is challenging due to intractable sequence-level likelihoods. Existing approaches therefore rely on surrogate likelihoods or heuristic approximations, which can introduce bias and obscure the sequential structure of denoising. We formulate diffusion-based sequence generation as a finite-horizon Markov decision process over the denoising trajectory and derive an exact, unbiased policy gradient that decomposes over denoising steps and is expressed in terms of intermediate advantages, without requiring explicit evaluation of the sequence likelihood. To obtain a practical and compute-efficient estimator, we (i) select denoising steps for policy updates via an entropy-guided approximation bound, and (ii) estimate intermediate advantages using a one-step denoising reward naturally provided by the diffusion model, avoiding costly multi-step rollouts. Experiments on coding and logical reasoning benchmarks demonstrate state-of-the-art results, with strong competitive performance on mathematical reasoning, outperforming existing RL post-training approaches for DLMs. Code is available at Github.

## 1. Introduction

Diffusion Language Models (DLMs) (Sahoo et al., 2024; Nie et al., 2025; Ye et al., 2025) have recently emerged as a compelling alternative to autoregressive language models (ARLMs). Instead of generating tokens sequentially from left to right, DLMs produce text through an iterative denoising process, typically via masked discrete diffusion, en-

abling bidirectional context and multi-token parallelism for higher token throughput while maintaining competitive output quality. These advantages have spurred rapid progress in DLM architectures and algorithms, including multimodal generation (Yang et al., 2025; Li et al., 2025), long-context modeling (Liu et al., 2025), accelerated inference (Wu et al., 2025), and code generation (Song et al., 2025). Motivated by the transformative impact of reinforcement learning (RL) post-training on ARLMs (Guo et al., 2025), there is now growing interest in developing effective and scalable RL algorithms tailored to DLMs.

Despite the success of RL post-training for ARLMs, extending these methods to DLMs is *not* a direct translation. RL for ARLMs relies on causal token-wise factorization, which yields a natural token-space Markov decision process (MDP) and enables efficient computation of log-likelihoods and importance ratios. DLMs fundamentally break this structure: generation proceeds through a denoising trajectory in masked space, and the likelihood of the final output does not admit a readily usable token-wise decomposition. As a result, naïvely porting standard policy-gradient objectives leads to intractable or prohibitively expensive likelihood evaluations. At the same time, diffusion generation offers opportunities largely absent in ARLMs. Model uncertainty evolves non-uniformly along the denoising trajectory, motivating *stepwise credit/advantage assignment* and *stepwise compute allocation* across diffusion steps. Moreover, masked DLMs output token distributions for all positions at each step, enabling a lightweight “full unmasking” that can serve as an increasingly accurate proxy of the eventual output later in the trajectory, and thus provide partial learning signals for intermediate steps without an explicit pretrained value function. Together, these challenges and opportunities motivate a principled approach to RL for DLMs that exploits diffusion structure.

A growing body of work has begun exploring RL post-training for diffusion LMs, largely via surrogate objectives and tractable likelihood approximations. *d1* (Zhao et al., 2025b) adapts GRPO to DLMs using mean-field likelihood approximations; *wd1* (Tang et al., 2025) modifies the objective to reduce instability while still relying

<sup>\*</sup>Equal contribution <sup>1</sup>Department of Electrical and Computer Engineering, Texas A&M university, College Station, Texas. Correspondence to: Dileep Kalathil <dileep.kalathil.tamu.edu>.

on proxy likelihoods; *SPG* (Wang et al., 2025a) optimizes pessimistic/optimistic bound-based surrogates; *d2* (Wang et al., 2025c) derives a trajectory-level formulation but employs step-merging estimators to obtain tractable updates; *TraceRL* (Wang et al., 2025d) introduces trajectory-aware training with a diffusion-based value model; and *DiFFPO* (Zhao et al., 2025a) proposes off-policy training via surrogate policies with improved likelihood approximations and importance sampling. While these methods are practically effective, they typically begin with a *chosen approximation* (to the likelihood, objective, or advantage) and optimize the resulting surrogate directly, leaving the connection to the true RL objective less explicit and step-level optimization across the denoising trajectory largely implicit.

We take a complementary, first-principles approach that makes the diffusion structure explicit, rather than treating a DLM as a black-box sampler. Instead of beginning with a particular surrogate likelihood approximation, we ask the fundamental questions that should underlie any principled RL method for diffusion LMs: What is the right MDP formalism for DLMs? What is the exact policy gradient for the true RL objective? How can it be approximated tractably at scale? And how can diffusion-time structure enable *stepwise* advantage (credit) estimation and *compute allocation* across denoising steps? We answer these questions in the affirmative, leading to the following main contributions.

- **MDP formalism for DLMs:** We formulate masked diffusion generation as a finite-horizon MDP over denoising steps, making the structure needed for RL explicit.
- **Exact policy gradient with stepwise advantage:** Building on the MDP formalism, we derive an *exact* policy-gradient theorem that decomposes over denoising steps, yielding a principled notion of *stepwise advantages*.
- **Tractable estimators exploiting diffusion structure:** We turn this exact theory into a practical algorithm by exploiting two DLM-native capabilities absent in ARLMs. First, we allocate training compute *across denoising steps* using the model’s intrinsic uncertainty: higher-entropy steps are prioritized under a fixed budget. We call this method **Entropy-Guided Stepwise Policy Optimization (EGSPO)**. Second, in addition to the entropy-guided step selection, we estimate stepwise advantages via a lightweight full-sequence “one-shot” completion from intermediate states, yielding intermediate learning signals without an extra value network or costly multi-step rollouts. We call this method **Entropy-Guided Stepwise Policy Optimization with Stepwise Advantages (EGSPO-SA)**. Together, these ideas make RL training scalable for DLMs while preserving the diffusion-time structure.
- **State-of-the-art results on coding/reasoning:** Empirically, we achieve state-of-the-art results on standard *cod-*

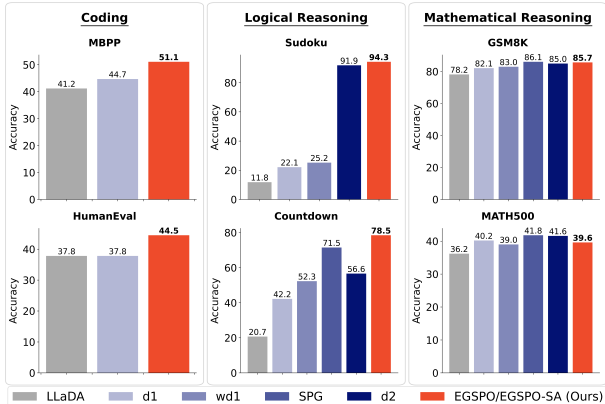


Figure 1. Overview of the performance on coding and reasoning tasks. Our approach outperforms the existing baselines in coding and logical reasoning tasks, while maintaining competitive performance in mathematical reasoning tasks.

*ing* and *logical reasoning* benchmarks, outperforming existing RL post-training approaches for DLMs.

## 2. Related Work

**Diffusion Language Models:** Diffusion language models (DLMs) (Sahoo et al., 2024; Nie et al., 2025; Ye et al., 2025) extend discrete diffusion frameworks (Austin et al., 2021a; Lou et al., 2023; Song et al., 2025) to natural language, enabling parallel multi-token generation. Prior work has explored architectural simplifications (Shi et al., 2024), theoretical connections between discrete and continuous diffusion (Zhao et al., 2024), and multimodal extensions (Yang et al., 2025; Li et al., 2025). Another line of research focuses on inference efficiency, including remasking schemes (Wang et al., 2025b), token reordering (Arriola et al., 2025; Sahoo et al., 2025), and entropy- or confidence-based sampling strategies (Ben-Hamu et al., 2025; Wu et al., 2025).

**RL for LLMs and Reasoning:** Reinforcement learning has become central to enhancing the reasoning capabilities of auto-regressive language models (ARLMs) (OpenAI, 2024), with policy-gradient methods such as PPO (Schulman et al., 2017) and GRPO (Shao et al., 2024) enabling effective fine-tuning on mathematical reasoning, coding, and planning tasks (Guo et al., 2025; Zhang et al., 2025).

**RL for Diffusion Image Models:** RL has also been applied to diffusion models for image generation, where rewards are commonly derived from pretrained classifiers, aesthetic metrics, or downstream task objectives. Prior work primarily adopts policy-gradient methods (Black et al., 2024; Fan et al., 2023; Uehara et al., 2024) or preference-based direct policy optimization (Wallace et al., 2024; Yang et al., 2024). These methods operate in continuous diffusion

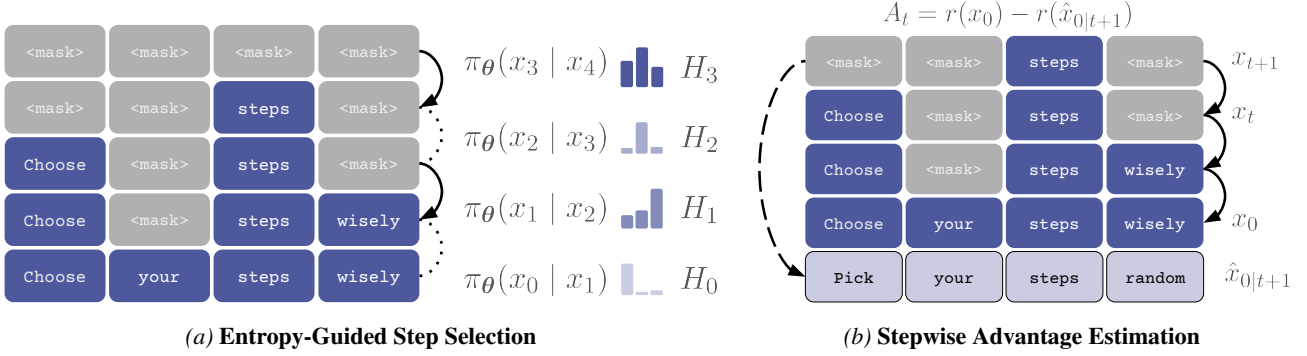


Figure 2. (a) Illustration of entropy-guided denoising step selection: At each denoising step  $t$ , the entropy  $H_t$  of the unmasking policy distribution is computed and used to identify the  $K$  informative steps that have maximum entropy. In the figure, assuming  $H_3 > H_1 > H_2 > H_0$  and  $K = 2$ , the two highest-entropy steps 3, 1 are selected for per-step policy gradient computation (marked by solid lines). (b) Illustration of stepwise advantage estimation: From state  $\mathbf{x}_{t+1}$ , a greedy one-step completion  $\hat{\mathbf{x}}_{0|t+1}$  provides a baseline reward approximating the state value. The stepwise advantage  $A_t$  measures the additional reward gained by taking the denoising action at step  $t$  and continuing to  $\mathbf{x}_0$ .

settings with dense rewards, unlike diffusion language models with discrete decisions and long-horizon sparse credit assignment.

### 3. Preliminaries and Problem Formulation

In this section, we provide a brief overview of the masked diffusion language model (MDLM) and reinforcement learning for language models.

**Notations.** Let  $\mathbf{x} = \mathbf{x}_{0:T,1:L}$  denote a sequence of  $T + 1$  steps of  $L$ -length sentences. Each of  $\mathbf{x}_t$  can take values from a finite set of vocabulary  $\mathcal{V} \cup \{\mathbf{m}\}$  where  $\mathbf{m}$  is a special token denoting mask. The state  $\mathbf{x}_0$  denotes the clean sentence and can take values only in  $\mathcal{V}$ .

#### 3.1. Masked Diffusion Language Models

The MDLMs (Sahoo et al., 2024; Nie et al., 2025; Song et al., 2025; Ye et al., 2025) involve a *forward masking* (noising) process and *reverse unmasking* (denoising). During the training, the masking process is implemented by taking a clean sequence  $\mathbf{x}_0 = \mathbf{x}_{0,1:L}$  and obtaining a partially masked sequence  $\mathbf{x}_t$  as

$$\mathbf{x}_{t,\ell} \sim q^{t|0}(\cdot | \mathbf{x}_{0,\ell}) = \text{Cat}(\cdot | \alpha_t \mathbf{x}_{0,\ell} + (1 - \alpha_t) \mathbf{m}),$$

where  $\alpha_t \in [0, 1]$  is a strictly decreasing noise schedule typically chosen to be  $\alpha_t = 1 - \frac{t}{T}$  for  $t \in [0, T - 1]$ .

The reverse unmasking process is parameterized by a neural network  $f_\theta$  that specifies the distribution over tokens at each position. Given a partially masked sequence at time  $t$  and for any  $s < t$ , the denoised sample is obtained as

$$\mathbf{x}_{s,\ell} \sim \pi_\theta^{s|t}(\cdot | \mathbf{x}_t) = q^{s|t,0}(\cdot | \mathbf{x}_t, \mathbf{x}_0 = f_\theta(\cdot | \mathbf{x}_t)). \quad (1)$$

In practice, a sample  $\mathbf{x}_s$  is obtained starting from  $\mathbf{x}_t$  iter-

atively as  $\pi_\theta^{s:t-1|t}(\mathbf{x}_{s:t-1} | \mathbf{x}_t) \triangleq \prod_{u=t-1}^s \pi_\theta^{u|u+1}(\mathbf{x}_u | \mathbf{x}_{u+1})$ . The complete reverse sampling process starts from  $\mathbf{x}_T$  and samples iteratively for  $t = T - 1, \dots, 0$ . Given  $\mathbf{x}_{t+1}$ , let  $M_t = M_t(\mathbf{x}_{t+1}) \triangleq \{\ell : \mathbf{x}_{t+1,\ell} = \mathbf{m}\}$  denote the set of masked positions. The positions to unmask are typically decided using some heuristic based on  $f_{\theta,\ell}(\cdot | \mathbf{x}_{t+1})$  for  $\ell \in M_t(\mathbf{x}_{t+1})$ . The diffusion LM model  $f_\theta$  is trained by minimizing the negative evidence lower bound (NELBO):

$$-\mathbb{E}_{\mathbf{x}_0 \sim p_{\text{data}}, \mathbf{x}_t \sim q^{t|0}(\cdot | \mathbf{x}_0)} \left[ \sum_{\ell=1}^{|\mathbf{x}_t|} \mathbb{I}_{\{\mathbf{x}_{t,\ell} = \mathbf{m}\}} \log f_{\theta,\ell}(\mathbf{x}_{0,\ell} | \mathbf{x}_t) \right].$$

This essentially means that  $f_\theta$  models a product distribution over the clean tokens in the masked position of the input sequence  $\mathbf{x}_t$ , which is equivalent to getting a probability distribution over  $\mathbf{x}_0$  given  $\mathbf{x}_t$ . We denote this one-step denoising distribution as  $\pi_\theta^{0|t}$ , given by

$$\pi_\theta^{0|t}(\mathbf{x}_0 | \mathbf{x}_t) = \prod_{\ell: \mathbf{x}_{t,\ell} = \mathbf{m}} f_{\theta,\ell}(\mathbf{x}_{0,\ell} | \mathbf{x}_t). \quad (2)$$

In the following, we drop the superscript that denotes the time steps in the policy  $\pi_\theta$  to lighten the notation.

#### 3.2. Reinforcement Learning for LLMs

Given a query  $\mathbf{q} \sim \mathcal{D}$ , an LM generates an output  $\mathbf{x}_0$  and receives a reward  $r(\mathbf{x}_0, \mathbf{q})$ . RL fine-tuning seeks to maximize the expected reward:

$$J(\theta) \triangleq \mathbb{E}_{\mathbf{q}, \mathbf{x}_0 \sim \pi_\theta(\cdot | \mathbf{q})} [r(\mathbf{x}_0, \mathbf{q})]. \quad (3)$$

Policy-gradient methods are standard tools for optimizing (3). Among them, the Group Relative Policy Optimization (GRPO) (Shao et al., 2024) is widely popular for RL with Verifiable Reward (RLVR) tasks, as it eliminates the need

for a trained value model used in PPO-style algorithms (Schulman et al., 2017). The GRPO loss function for an auto-regressive (AR) LM is given by

$$L_{\text{AR}}(\boldsymbol{\theta}) = -\mathbb{E}_{\mathbf{q}, \mathbf{x}_0 \sim \pi_{\boldsymbol{\theta}_{\text{old}}}(\cdot | \mathbf{q})} \left[ \frac{1}{L} \sum_{\ell=1}^L \min(\rho_{\ell} A^{\pi_{\boldsymbol{\theta}_{\text{old}}}}, \text{clip}(\rho_{\ell}, 1 - \epsilon, 1 + \epsilon) A^{\pi_{\boldsymbol{\theta}_{\text{old}}}}) \right] + \beta D_{\text{KL}}(\pi_{\boldsymbol{\theta}} \| \pi_{\text{ref}}) \quad (4)$$

where  $\pi_{\boldsymbol{\theta}_{\text{old}}}$  denotes the sampling policy,  $\rho_{\ell} = \frac{\pi_{\boldsymbol{\theta}}(\mathbf{x}_{0,\ell} | \mathbf{x}_{0,<\ell}, \mathbf{q})}{\pi_{\boldsymbol{\theta}_{\text{old}}}(\mathbf{x}_{0,\ell} | \mathbf{x}_{0,<\ell}, \mathbf{q})}$  denotes the per-token importance ratio,  $\beta$  controls the strength of the KL regularization w.r.t. the base model  $\pi_{\text{ref}}$ , and the advantage  $A^{\pi_{\boldsymbol{\theta}}}$  is defined for any policy  $\pi_{\boldsymbol{\theta}}$  as

$$A^{\pi_{\boldsymbol{\theta}}}(\mathbf{x}_0, \mathbf{q}) = r(\mathbf{x}_0, \mathbf{q}) - \mathbb{E}_{\mathbf{x}_0 \sim \pi_{\boldsymbol{\theta}}(\cdot | \mathbf{q})} [r(\mathbf{x}_0, \mathbf{q})], \quad (5)$$

which is approximated by a Monte Carlo estimate. More precisely, for a given query  $\mathbf{q}$ , we sample  $\mathbf{x}^j \sim \pi_{\boldsymbol{\theta}_{\text{old}}}(\cdot | \mathbf{q})$ ,  $1 \leq j \leq G$ , and estimate

$$A^{\pi_{\boldsymbol{\theta}_{\text{old}}}}(\mathbf{x}_0^j, \mathbf{q}) = r(\mathbf{x}_0^j, \mathbf{q}) - \frac{1}{G} \sum_{i=1}^G r(\mathbf{x}_0^i, \mathbf{q}). \quad (6)$$

A *well-known limitation* of GRPO is that the same sequence-level advantage  $A^{\pi_{\boldsymbol{\theta}_{\text{old}}}}$  is broadcast to all tokens, whereas PPO-style methods can (in principle) use token-specific advantages via a learned value function. This *credit assignment* issue becomes substantially more pronounced for diffusion LMs, where decision-making occurs over denoising steps rather than token positions.

### 3.3. Problem Formulation: RL for Diffusion LLMs

RL finetuning of an AR-LLM exploits its auto-regressive structure by modeling the token generation as a token-space MDP, and the LLM as a policy. Since  $\mathbf{x}_0 = \mathbf{x}_{0,1:L}$ , we can define the initial state as  $\mathbf{q}$ , state at step  $\ell$  as  $(\mathbf{q}, \mathbf{x}_{0,<\ell})$  and action at step  $\ell$  as the next token  $\mathbf{x}_{0,\ell} \sim \pi_{\boldsymbol{\theta}}(\cdot | \mathbf{x}_{0,<\ell}, \mathbf{q})$ . This MDP formalism offers a significant computational advantage in training, because any policy gradient algorithm for solving (3) has to calculate the term  $\pi_{\boldsymbol{\theta}}(\mathbf{x}_0 | \mathbf{q})$ , and here it decomposes as  $\pi_{\boldsymbol{\theta}}(\mathbf{x}_0 | \mathbf{q}) = \prod_{\ell=1}^L \pi_{\boldsymbol{\theta}}(\mathbf{x}_{0,\ell} | \mathbf{x}_{0,<\ell}, \mathbf{q})$ . Due to causal attention of AR-LLM, all these terms can be efficiently computed using only a single model forward pass. Unfortunately, diffusion LMs break these conveniences because there is no token-wise causal factorization of  $\pi_{\boldsymbol{\theta}}(\mathbf{x}_0 | \mathbf{q})$  available at training time. As a consequence, naively porting the RL training objectives for AR-LLM, such as Eq. (4), would require evaluating (explicitly or implicitly) sequence-level likelihood terms that are intractable or prohibitively expensive for diffusion models.

Recent work has made progress on RL for diffusion LMs by introducing surrogate objectives and likelihood approximations. Representative examples include: (i) mean-field or

one-step likelihood approximations to enable GRPO-style ratios (Zhao et al., 2025b); (ii) ratio-free weighted updates that still rely on tractable proxy likelihoods (Tang et al., 2025); (iii) pessimistic bound-based objectives that optimize lower/upper bounds on likelihood quantities (Wang et al., 2025a); and (iv) trajectory-based formulations with biased step-merging estimators or additional structural assumptions for one-pass evaluation (Wang et al., 2025c). These approaches are practical, but they necessarily make compromises: the optimized objective may deviate from 3, the resulting gradients may be biased, and, crucially, the role of *individual denoising steps* in producing the final reward is often ignored.

In this work, we take a complementary approach. Rather than beginning with a particular surrogate likelihood approximation, we ask the foundational questions that should underlie any principled RL method for diffusion LMs.

(i) *MDP formalism*: What are the states, actions, and transitions that faithfully represent diffusion-based generation while remaining amenable to RL analysis?

(ii) *Policy-gradient for Eq. (3)*: Can we derive an *unbiased* gradient expression that respects the sequential structure of denoising? How can we estimate that gradient tractably?

(iii) *Stepwise advantages*: In AR decoding, actions are tied to token positions; in diffusion decoding, actions are tied to denoising step. Can diffusion structure yield improved stepwise advantages that do not have direct AR analogues?

We provide positive answers to these questions in Section 4.

## 4. Methodology

### 4.1. Diffusion MDP and Policy Gradient Theorem

We formalize the unmasking process as a  $T$ -step MDP. The state and action at time  $t$  is defined as  $\mathbf{s}_t = (\mathbf{x}_{T-t}, \mathbf{q})$  and  $\mathbf{a}_t = \mathbf{x}_{T-t-1}$ . The transition probability function is deterministic by construction. The reward at time  $t$  is given by  $r_t = 0$  for all  $t < T$  and  $r_T(\mathbf{s}_T) = r(\mathbf{x}_0, \mathbf{q})$ . Notice that the time index moves forward in the MDP, but it moves backwards in the diffusion process. To keep the notation consistent, we only use the time index corresponding to the diffusion in defining the quantities of interest.

The value of a policy  $\pi$  at time step  $t$  is given by

$$V_t^{\pi}(\mathbf{x}_t, \mathbf{q}) = \mathbb{E}_{\mathbf{x}_{<t} \sim \pi^{<t|t}(\cdot | \mathbf{x}_t, \mathbf{q})} [r(\mathbf{x}_0, \mathbf{q})], \quad (7)$$

where  $\mathbf{x}_{<t} \sim \pi^{<t|t}(\cdot | \mathbf{x}_t, \mathbf{q})$  denotes that the expectation is with respect to the trajectories that start at  $\mathbf{x}_t$  and generate  $\mathbf{x}_0$  in  $t$  steps. The value of a policy  $V^{\pi}$ , averaged over the initial state, is then defined as  $V^{\pi} = \mathbb{E}_{\mathbf{q}} [V_T^{\pi}(\mathbf{m}, \mathbf{q})]$ . By comparing Eq. (3) and Eq. (7), it is straightforward to see that  $J(\boldsymbol{\theta}) = V^{\pi_{\boldsymbol{\theta}}}$ , showing that our MDP formalism will indeed solve the finetuning problem.

We now derive the policy gradient theorem for the diffusion MDP.

**Theorem 1** (Policy Gradient Theorem). *The gradient of the objective  $J(\theta)$  (c.f. Eq. (3)) is given by*

$$\begin{aligned} \nabla_{\theta} J(\theta) &= \mathbb{E}_{\mathbf{q}, \mathbf{x} \sim \pi_{\theta}(\cdot | \mathbf{q})} [r(\mathbf{x}_0, \mathbf{q}) \nabla_{\theta} \log \pi_{\theta}(\mathbf{x} | \mathbf{q})] \quad (8) \\ &= \sum_{t=0}^{T-1} \mathbb{E}_{\mathbf{q}, \mathbf{x} \sim \pi_{\theta}} [A_t^{\pi_{\theta}}(\mathbf{x}_{t+1}, \mathbf{x}_0, \mathbf{q}) \nabla_{\theta} \log \pi_{\theta}(\mathbf{x}_t | \mathbf{x}_{t+1})], \quad (9) \end{aligned}$$

where the step-level advantage is given by

$$A_t^{\pi_{\theta}}(\mathbf{x}_{t+1}, \mathbf{x}_0, \mathbf{q}) \triangleq r(\mathbf{x}_0, \mathbf{q}) - V_{t+1}^{\pi_{\theta}}(\mathbf{x}_{t+1}, \mathbf{q}). \quad (10)$$

The proof is given in Appendix A.

*Remark 2.* In the expression for policy gradient, we have the step-level score function given by  $\nabla_{\theta} \log \pi_{\theta}(\mathbf{x}_t | \mathbf{x}_{t+1})$ . To write this in terms of the trained model  $f_{\pi_{\theta}}$ , defining the set of unmasked tokens at time  $t$  as  $U_t = U_t(\mathbf{x}_t, \mathbf{x}_{t+1}) \triangleq \{\ell : \mathbf{x}_{t,\ell} \neq \mathbf{x}_{t+1,\ell}\}$ , we can write

$$\begin{aligned} \log \pi_{\theta}(\mathbf{x}_t | \mathbf{x}_{t+1}) &= \log \pi_{\theta}(\mathbf{x}_t, U_t | \mathbf{x}_{t+1}) \\ &= \log \pi_{\theta}(U_t | \mathbf{x}_{t+1}) + \log \pi_{\theta}(\mathbf{x}_t | \mathbf{x}_{t+1}, U_t) \\ &= \log \pi_{\theta}(U_t | \mathbf{x}_{t+1}) + \sum_{\ell \in U_t} \log f_{\theta}(\mathbf{x}_{t,\ell} | \mathbf{x}_{t+1}). \end{aligned}$$

If the set of positions to unmask  $U_t$  is chosen independently of  $\theta$ , then the score function can be computed as

$$\nabla_{\theta} \log \pi_{\theta}(\mathbf{x}_t | \mathbf{x}_{t+1}) = \sum_{\ell \in U_t} \nabla_{\theta} \log f_{\theta}(\mathbf{x}_{t,\ell} | \mathbf{x}_{t+1}). \quad (11)$$

Practical schemes use confidence-based decoding, where  $\ell \in U_t$  if  $\max_{\mathbf{x}_{t,\ell}} \log f_{\theta}(\mathbf{x}_{t,\ell} | \mathbf{x}_{t+1})$  is large among all masked positions  $\ell$ . Thus, aligning with Eq. (11), we can use  $\pi(\mathbf{x}_t | \mathbf{x}_{t+1}) = \prod_{\ell \in U_t(\mathbf{x}_t, \mathbf{x}_{t+1})} f_{\pi, \ell}(\mathbf{x}_{t,\ell} | \mathbf{x}_{t+1})$  for the policy optimization.

## 4.2. Entropy-Guided Step Selection

In AR-LLMs, given a sequence  $\mathbf{x}_0$ , the network output at position  $\ell$  models the likelihood  $\pi_{\theta}(\mathbf{x}_{0,\ell} | \mathbf{x}_{0,<\ell})$  for all  $\ell \in [1 : L]$  due to the causal attention mask. Thus, a single forward pass gives all the required likelihoods. This convenience is broken in diffusion LM due to its bidirectional attention, and it can compute only the term  $\pi_{\theta}(\mathbf{x}_t | \mathbf{x}_{t+1})$  in the forward pass of  $f_{\theta}(\cdot | \mathbf{x}_{t+1})$ . The policy gradient in Eq. (9) has  $T$  such terms, each requiring a separate forward pass through the network. This is computationally expensive as  $T$  is typically of the order of  $10^2 - 10^3$ .

To overcome this challenge, we wish to take the gradient only at a subset  $S$  of the time-steps of size at most

$K \leq T$ . Defining the per-step gradient as  $\nabla_{\theta} J_t(\theta) = \mathbb{E}_{\mathbf{q}, \mathbf{x} \sim \pi_{\theta}(\cdot | \mathbf{q})} [A_t^{\pi_{\theta}}(\mathbf{x}_{t+1}, \mathbf{x}_0, \mathbf{q}) \nabla_{\theta} \log \pi_{\theta}(\mathbf{x}_t | \mathbf{x}_{t+1})]$ , we can write  $\nabla_{\theta} J(\theta) = \sum_{t=0}^{T-1} \nabla_{\theta} J_t(\theta)$ . For a chosen subset  $S$ , we evaluate the policy gradient as

$$\nabla_{\theta} J_S(\theta) = \sum_{t \in S} \nabla_{\theta} J_t(\theta). \quad (12)$$

Two intuitive heuristics to choose this subset are:

- (i) *Random:*  $S = \text{choose}[K]\{t \sim \text{random}[0 : T - 1]\}$
- (ii) *Uniform:*  $S = \{kT/K : k \in [0 : K - 1]\}$ .

However, these approaches overlook the structure of the policy at each denoising step along the trajectory. A more principled approach would be to choose  $S$  with  $|S| \leq K$  such that error  $\Delta_S = \|J(\theta) - J_S(\theta)\|$  is minimized. Since evaluating this objective  $\Delta_S$  directly is expensive, we instead minimize a surrogate objective.

**Lemma 3.** *Let  $\pi_{\theta}^{t|t+1}$  be the softmax policy with logits  $g_{\theta}^{t,i}$  over  $i \in |\mathcal{V}|$  for each  $t \in [0 : T - 1]$ . Let  $\|\nabla_{\theta} g_{\theta}^t\| \triangleq \max_{i,j} \|\nabla_{\theta} (g_{\theta}^{t,i} - g_{\theta}^{t,j})\|$  and assume that  $\max_t \|\nabla_{\theta} g_{\theta}^t\| \leq B$ . Suppose the advantages  $A_t^{\pi_{\theta}}$  are uniformly bounded by 1. Defining  $\Delta_S = \|J(\theta) - J_S(\theta)\|$ , we have*

$$\Delta_S \leq B \sum_{t \notin S} H(\pi_{\theta}^{t|t+1}), \quad (13)$$

where  $H(\pi_{\theta}^{t|t+1})$  denotes the entropy of  $\pi_{\theta}(\cdot | \mathbf{x}_{t+1})$ .

Proof is given in Section A.

Using the upperbound in Eq. (13) as the surrogate objective for  $\Delta_S$ , we solve the following optimization problem to select time steps:

$$\min_{S \subseteq [0:T-1]} \sum_{t \notin S} H(\pi_{\theta}^{t|t+1}), \quad |S| \leq K. \quad (14)$$

The solution of (14) is given by the greedy choice:

$$S^* = \text{top}[K](t : H(\pi_{\theta}^{t|t+1})) \quad (15)$$

Intuitively, at these steps, the model is less confident about unmasking the next position. So, it is reasonable to allocate the gradient computation to these steps to reduce the uncertainty and improve the overall accuracy.

## 4.3. Estimating Stepwise Advantages

To compute the advantage  $A_t^{\pi_{\theta}}$ , we need to evaluate the baseline value  $V_t^{\pi_{\theta}}(\mathbf{x}_t, \mathbf{q})$  (c.f. Eq. (7)). Evaluating this using Monte Carlo sampling will require generating multiple trajectories that start at  $\mathbf{x}_t$  and reach  $\mathbf{x}_0$  in  $t$  steps, which requires a significant number of additional forward passes through the model, and thus makes it impractical. To overcome this difficulty, we leverage the structure of the diffusion LM:  $f_{\theta}$  models a product distribution over the

clean tokens in the masked position of the input sequence  $\mathbf{x}_t$ , which is equivalent to getting a probability distribution over  $\mathbf{x}_0$  given  $\mathbf{x}_t$ . In Eq. (2), we defined this one-step denoising distribution as  $\pi_{\theta}^{0|t}$ . Using this, we propose an approximation to the  $V_t^{\pi_{\theta}}$  as,

$$\hat{V}_t^{\pi_{\theta}}(\mathbf{x}_t, \mathbf{q}) = \mathbb{E}_{\mathbf{x}_0 \sim \pi_{\theta}^{0|t}(\cdot|\mathbf{x}_t, \mathbf{q})}[r(\mathbf{x}_0, \mathbf{q})]. \quad (16)$$

The above approximation will introduce a bias when  $t$  is large (beginning of the generation) due to the mismatch between  $t$ -step  $\pi_{\theta}^{<t|t}$  and 1-step denoising  $\pi_{\theta}^{0|t}$ . As  $t$  becomes small, i.e., towards the end of the generation process, the above bias becomes smaller, and we get accurate estimates of the value function. To account for the bias, in practical implementation, we estimate the advantages with a hyperparameter  $\lambda_t \in [0, 1]$ :

$$\hat{A}_t^{\pi_{\theta}} = (1 + \lambda_t)r(\mathbf{x}_0, \mathbf{q}) - \lambda_t \hat{V}_{t+1}^{\pi_{\theta}}(\mathbf{x}_{t+1}, \mathbf{q}). \quad (17)$$

#### 4.4. From Policy Gradient to GRPO Loss

Combining the results from Section 4.1–Section 4.3, we can define a GRPO loss with the stepwise advantages as

$$L(\theta; \theta_{\text{old}}) = \mathbb{E}_{\mathbf{q}, \mathbf{x} \sim \pi_{\theta_{\text{old}}}(\cdot|\mathbf{q})}[\sum_{t \in S} L_t], \quad (18)$$

where  $L_t$  is the per-step clipped surrogate loss with KL regularization given by

$$L_t = -\min(\rho_t A_t, \text{clip}(\rho_t, 1 - \epsilon, 1 + \epsilon) A_t) + \beta D_{\text{KL}}(\pi_{\theta}(\cdot | \mathbf{x}_{t+1}) \| \pi_{\text{ref}}(\cdot | \mathbf{x}_{t+1})), \quad (19)$$

where  $\rho_t = \frac{\pi_{\theta}(\mathbf{x}_t | \mathbf{x}_{t+1})}{\pi_{\theta_{\text{old}}}(\mathbf{x}_t | \mathbf{x}_{t+1})}$ , and  $A_t = \hat{A}_t^{\pi_{\theta_{\text{old}}}}(\mathbf{x}_{t+1}, \mathbf{x}_0, \mathbf{q})$ .

Suppose there is no clipping ( $\epsilon = \infty$ ), no KL term ( $\beta = 0$ ), and  $S = [0 : T - 1]$  all the time steps, then it can be easily shown that  $\nabla_{\theta} J(\theta)|_{\theta=\theta_{\text{old}}} = -\nabla_{\theta} L(\theta; \theta_{\text{old}})|_{\theta=\theta_{\text{old}}}$ , resulting in the right direction of policy optimization.

**Practical Implementation:** For a query  $\mathbf{q} \sim \mathcal{D}$ , we sample completions  $\mathbf{x}^j \sim \pi_{\theta_{\text{old}}}(\cdot | \mathbf{q})$  for  $j = 1, \dots, G$ . Then, we compute the stepwise advantages

$$\hat{A}_t^{\pi_{\theta_{\text{old}}}}(\mathbf{x}^j, \mathbf{q}) = (1 + \lambda_t)r(\mathbf{x}_0^j, \mathbf{q}) - \lambda_t r(\hat{\mathbf{x}}_0(\mathbf{x}_{t+1}^j), \mathbf{q}),$$

where  $\hat{\mathbf{x}}_0(\mathbf{x}_{t+1}^j)$  is the greedy completion corresponding to one-step denoising distribution, i.e.,

$$\hat{\mathbf{x}}_{0, \ell}(\mathbf{x}_{t+1}^j) = \begin{cases} \arg \max_v f_{\theta_{\text{old}}, \ell}(v | \mathbf{x}_{t+1}^j), & \mathbf{x}_{t+1, \ell}^j = \mathbf{m} \\ \mathbf{x}_{t+1, \ell}^j, & \text{otherwise,} \end{cases} \quad (20)$$

which is a further approximation to Eq. (17), replacing the expectation of the reward with the reward of the greedy

completion. Finally, to reduce the variance, we use centered advantages:

$$\hat{A}_t^{\pi_{\theta_{\text{old}}}}(\mathbf{x}^j, \mathbf{q}) = \hat{A}_t^{\pi_{\theta_{\text{old}}}}(\mathbf{x}^j, \mathbf{q}) - \frac{1}{G} \sum_{i=1}^G \hat{A}_t^{\pi_{\theta_{\text{old}}}}(\mathbf{x}^i, \mathbf{q}),$$

for the advantages in GRPO loss. We pick  $S$  based on  $H(\pi_{\theta_{\text{old}}}^{t|t+1})$ , which can be computed for each  $t$  during the rollout phase without additional compute (see Section 4.2).

With the proposed step-selection strategy and stepwise advantage estimation, we refer to our method as *Entropy-Guided Stepwise Policy Optimization with Stepwise Advantages (EGSPO-SA)*. Setting  $\lambda_t = 0$  recovers entropy-guided step selection with vanilla group-relative sequence advantages, which we denote as *EGSPO*.

## 5. Experimental Results

All experiments are conducted using LLaDA-8B-Instruct, a masked diffusion language model, as the base model. Fine-tuning is performed without supervised fine-tuning (SFT). Additional experimental details are provided in the Appendix C.

We evaluate EGSPO and EGSPO-SA on a range of downstream reasoning tasks, including mathematical benchmarks (GSM8K (Cobbe et al., 2021), MATH500 (Lightman et al., 2023)), logical reasoning tasks (Sudoku and Countdown (Ye et al., 2024)), and coding benchmarks (MBPP (Austin et al., 2021b), HumanEval (Chen, 2021)). Across all benchmarks, we adopt the same terminal reward functions as used in prior work; detailed reward definitions are provided in Appendix B.

For mathematical and logical reasoning tasks, we report published results from prior work rather than re-implementing d1 (Zhao et al., 2025b), d2 (Wang et al., 2025c), wd1 (Tang et al., 2025), and SPG (Wang et al., 2025a). For coding tasks, reported baseline results are available only for d1 (Zhao et al., 2025b).

### 5.1. Main Results

Tables 1 and 2 report the test-time performance of EGSPO and EGSPO-SA across all tasks and generation lengths. Both methods consistently improve over the base *LLaDA-8B-Instruct* model, demonstrating the effectiveness of entropy-guided reinforcement learning for diffusion language models.

On logical reasoning benchmarks, including Countdown and Sudoku, EGSPO and EGSPO-SA substantially outperform prior diffusion-based RL approaches, with EGSPO-SA achieving the strongest overall performance. These tasks impose strict global constraints on intermediate decisions, and the observed gains suggest that step-level credit assignment

Entropy-Guided Stepwise Policy Optimization with Stepwise Advantages

Model / Seq. Len.	Sudoku				Countdown				GSM8K				MATH500			
	128	256	512	Best	128	256	512	Best	128	256	512	Best	128	256	512	Best
LLaDA-8B-Instruct	11.7	6.7	5.5	11.7	20.7	19.5	16.0	20.7	68.7	76.7	78.2	78.2	26.0	32.4	36.2	36.2
d1	22.1	16.7	9.5	22.1	34.8	32.0	42.2	42.2	73.2	81.1	82.1	82.1	<b>33.8</b>	<u>38.6</u>	<u>40.2</u>	40.2
wd1	-	76.4	62.8	76.4	-	51.2	46.1	51.2	-	80.8	82.3	82.3	-	34.4	39.0	39.0
SPG	82.9 <sup>†</sup>	94.0 <sup>†</sup>	93.1 <sup>†</sup>	94.0 <sup>†</sup>	68.8	71.5	70.3	71.5	<b>78.5</b>	<b>86.1</b>	84.5	<b>86.1</b>	<u>33.4</u>	<b>40.0</b>	<u>41.8</u>	<b>41.8</b>
d2				91.9				56.6				85.0				<u>41.6</u>
EGSPO (Ours)	<u>93.3</u>	<u>93.6</u>	<u>89.1</u>	<u>93.6</u>	<u>70.3</u>	<u>71.5</u>	<u>75.8</u>	<u>75.8</u>	<u>77.5</u>	<u>85.7</u>	<u>84.98</u>	<u>85.7</u>	32.2	37.8	39.0	39.0
EGSPO-SA (Ours)	<b>93.7</b>	<b>94.3</b>	<b>93.4</b>	<b>94.3</b>	<b>78.5</b>	<b>77.3</b>	<b>76.5</b>	<b>78.5</b>	73.5	84.6	<b>85.03</b>	85.03	33.2	38.2	39.6	39.6

Table 1. Main results across reasoning benchmarks. For each method, we report accuracy at different generation lengths and the best performance across lengths. d2 reports a single best performance independent of generation length, following its original evaluation protocol. wd1 does not report the evaluation on length 128. For Sudoku, <sup>†</sup> denotes 3-shot evaluation, whereas ours is 0-shot.

HumanEval	128	256	512	Best
LLaDA-8B-Instruct	27.4	35.3	37.8	37.8
d1	31.1	32.9	37.8	37.8
EGSPO (Ours)	<u>32.3</u>	<u>40.2</u>	<u>39.6</u>	<u>40.2</u>
EGSPO-SA (Ours)	<b>32.3</b>	<b>41.5</b>	<b>44.5</b>	<b>44.5</b>
MBPP	128	256	512	Best
LLaDA-8B-Instruct	36.2	41.2	40.4	41.2
d1	40.5	44.7	42.8	44.7
EGSPO (Ours)	49.9	<b>50.6</b>	<b>50.3</b>	<u>50.6</u>
EGSPO-SA (Ours)	<b>51.1</b>	<u>48.7</u>	<u>49.2</u>	<b>51.1</b>

Table 2. Results on coding benchmarks. We report accuracy at different generation lengths and the best performance across lengths.

is particularly beneficial in this setting.

On mathematical reasoning benchmarks (GSM8K and MATH500), both EGSPO and EGSPO-SA achieve performance comparable to prior diffusion-based RL methods, while consistently improving over the base model. In this regime, the additional gains from incorporating stepwise advantages are limited, indicating that the learning signal is largely captured by sequence-level advantages.

On coding benchmarks (MBPP and HumanEval), both EGSPO and EGSPO-SA outperform the available baselines across the evaluated generation lengths, with EGSPO-SA achieving the strongest overall results. These findings highlight not only the effectiveness of entropy-guided optimization for program synthesis, but also the importance of stepwise credit assignment, which helps identify and reinforce informative denoising steps where the model remains uncertain about its decisions.

We further analyze the dynamics of EGSPO and EGSPO-SA using the training curves shown in Figure 4. While both methods exhibit similar convergence behavior on mathematical reasoning tasks, EGSPO-SA consistently achieves

higher final performance and earlier learning onset on logical reasoning benchmarks. This effect is most pronounced on Sudoku, where EGSPO-SA begins improving substantially earlier and reaches higher reward more quickly.

**Compute Efficiency.** As shown in Figure 3, we compare EGSPO-SA and d1 on three compute axes. Reward vs. FLOPs measures the total floating-point operations accumulated across all forward passes during training. Reward vs. Samples counts the cumulative number of prompt-completion pairs generated during training, reflecting how many environment interactions each method requires. Reward vs. Gradient Steps counts the number of optimizer updates, reflecting how many weight updates each method needs to converge. Across all three axes, EGSPO-SA converges to near-perfect reward while d1 plateaus well below 0.2, demonstrating that EGSPO-SA is strictly more efficient in compute, data, and optimization.

## 5.2. Ablation Study

We conduct ablation studies to evaluate the contribution of individual components in the proposed method. All ablations are performed on the Sudoku.

**Effect of Entropy-Based Step Selection.** We compare *uniform*, *random*, and *entropy-based* step selection (EGSPO) under a fixed budget of  $K$  denoising steps per trajectory. Uniform selection (USPO) samples evenly spaced timesteps, random selection (RSPO) samples  $K$  steps uniformly at random, and entropy-based selection chooses the  $K$  steps with the highest average unmasking token entropy across timesteps.

As shown in Figure 5a, entropy-based selection achieves higher final performance and converges more rapidly under matched compute budgets. Uniform selection consistently outperforms random selection as training progresses, indicating that evenly covering the denoising trajectory provides more stable and informative updates than stochastic.

## Entropy-Guided Stepwise Policy Optimization with Stepwise Advantages

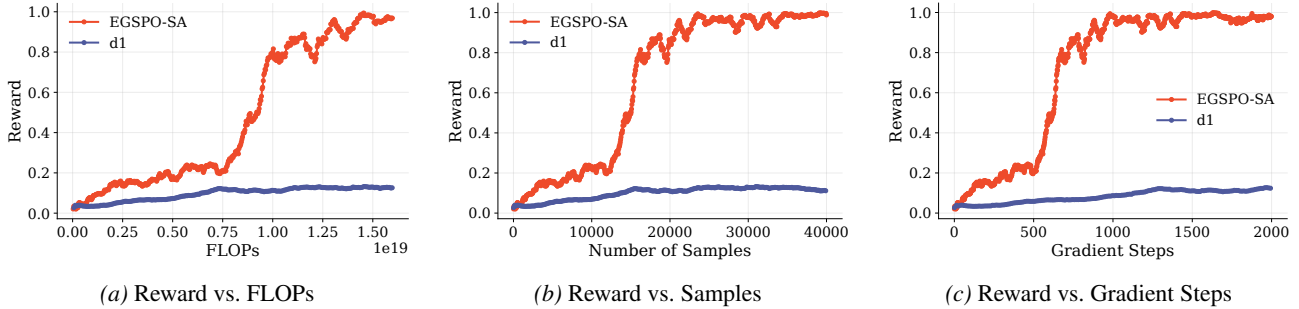


Figure 3. Compute efficiency comparison between EGSP0-SA and d1 on Sudoku. (a) FLOPs are accumulated over all forward passes across 8 GPUs. (b) Samples count cumulative prompt-completion pairs seen during training. (c) Gradient steps count optimizer updates (accounting for gradient accumulation). EGSP0-SA dominates d1 under all three compute budgets.

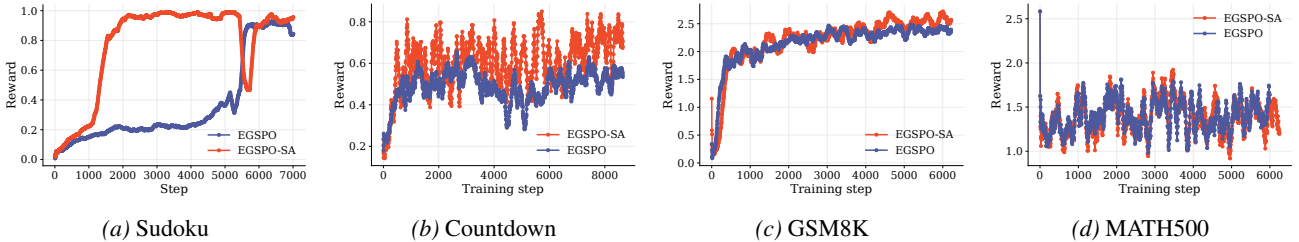


Figure 4. Training curves for EGSP0 and EGSP0-SA on Sudoku, Countdown, GSM8K, and MATH500 using the training settings described in Section C.

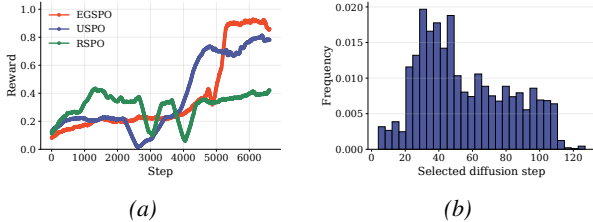


Figure 5. Ablation studies analyzing (a) entropy-guided step selection (EGSP0) versus uniform step selection (USPO) and (b) the distribution of selected steps.

By avoiding low-entropy, near-deterministic steps while maintaining coverage, entropy-based selection further concentrates updates on timesteps with stronger learning signal, consistent with the analysis in Section 4.2.

**Distribution of Selected Denoising Steps.** Figure 5b shows the distribution of denoising timesteps selected by entropy-based selection. Contrary to the expectation that early, heavily masked steps would dominate, selected steps span the diffusion horizon with a modest concentration on intermediate timesteps.

Early steps tend to produce diffuse predictions despite heavy masking, as the model is relatively certain about the broad set of admissible token choices. In contrast, intermediate steps correspond to a regime where partial structure has formed but multiple competing completions remain plausi-

ble, leading to higher uncertainty in token predictions. Late steps are largely deterministic and therefore selected less frequently. Overall, entropy-based selection emphasizes timesteps where the model is most uncertain about token assignments, rather than those that are simply more masked.

## 6. Conclusion

In this work, we introduced a principled reinforcement learning framework for diffusion language models that makes the denoising structure explicit rather than relying on surrogate likelihoods or heuristic objectives. By formulating masked diffusion generation as a finite-horizon Markov decision process over denoising steps, we derived an exact and unbiased policy gradient that decomposes naturally along the diffusion trajectory and yields a well-defined notion of stepwise advantages, without requiring explicit evaluation of intractable sequence-level likelihoods.

Building on this foundation, we proposed practical and scalable estimators that exploit diffusion-specific structure, including entropy-guided step selection for adaptive compute allocation and lightweight one-step denoising completions for intermediate advantage estimation. These components enable efficient stepwise policy optimization while preserving the theoretical guarantees of the underlying objective. Empirical results on coding and logical reasoning benchmarks demonstrate consistent improvements over existing RL post-training methods for diffusion language models.

## 7. Acknowledgments

Portions of this research were conducted with the advanced computing resources provided by Texas A&M High Performance Research Computing. This work was supported, in part, by National Science Foundation (NSF) under grants CNS-2148354, FuSe2-2425399, U.S. Army Combat Capabilities Development Command (DEVCOM) under Grant Number W911NF2520046. This work was also supported in part by the National Science Foundation grant NSF-CNS 2148354, federal agencies, and industry partners as specified in the Resilient & Intelligent NextG Systems (RINGS) program. Any opinions, findings, and conclusions or recommendations expressed in this material are those of the authors and do not necessarily reflect the views of the sponsoring agencies.

## References

- Arriola, M., Gokaslan, A., Chiu, J. T., Yang, Z., Qi, Z., Han, J., Sahoo, S. S., and Kuleshov, V. Block diffusion: Interpolating between autoregressive and diffusion language models. *arXiv preprint arXiv:2503.09573*, 2025.
- Austin, J., Johnson, D. D., Ho, J., Tarlow, D., and van den Berg, R. Structured denoising diffusion models in discrete state-spaces. In *Advances in Neural Information Processing Systems (NeurIPS)*, 2021a.
- Austin, J., Odena, A., Nye, M., Bosma, M., Michalewski, H., Dohan, D., Jiang, E., Cai, C., Terry, M., Le, Q., et al. Program synthesis with large language models. *arXiv preprint arXiv:2108.07732*, 2021b.
- Ben-Hamu, H., Gat, I., Severo, D., Nolte, N., and Karrer, B. Accelerated sampling from masked diffusion models via entropy bounded unmasking. In *Advances in Neural Information Processing Systems (NeurIPS)*, 2025.
- Black, K., Janner, M., Du, Y., Kostrikov, I., and Levine, S. Training diffusion models with reinforcement learning. In *International Conference on Learning Representations (ICLR)*, 2024.
- Chen, M. Evaluating large language models trained on code. *arXiv preprint arXiv:2107.03374*, 2021.
- Cobbe, K., Kosaraju, V., Bavarian, M., Chen, M., Jun, H., Kaiser, L., Plappert, M., Tworek, J., Hilton, J., Nakano, R., et al. Training verifiers to solve math word problems. *arXiv preprint arXiv:2110.14168*, 2021.
- Fan, Y., Watkins, O., Du, Y., Liu, H., Ryu, M., Boutilier, C., Abbeel, P., Ghavamzadeh, M., Lee, K., and Lee, K. DPOK: Reinforcement learning for fine-tuning text-to-image diffusion models. *Advances in Neural Information Processing Systems (NeurIPS)*, 2023.
- Guo, D., Yang, D., Zhang, H., Song, J., Zhang, R., Xu, R., Zhu, Q., Ma, S., Wang, P., Bi, X., et al. Deepseek-r1: Incentivizing reasoning capability in LLMs via reinforcement learning. *arXiv preprint arXiv:2501.12948*, 2025.
- Li, S., Kallidromitis, K., Bansal, H., Gokul, A., Kato, Y., Kozuka, K., Kuen, J., Lin, Z., Chang, K.-W., and Grover, A. LaViDa: A Large Diffusion Model for Vision-Language Understanding. In *Advances in Neural Information Processing Systems (NeurIPS)*, 2025.
- Lightman, H., Kosaraju, V., Burda, Y., Edwards, H., Baker, B., Lee, T., Leike, J., Schulman, J., Sutskever, I., and Cobbe, K. Let’s verify step by step. In *International Conference on Learning Representations (ICLR)*, 2023.
- Liu, X., Song, Y., Liu, Z., Huang, Z., Guo, Q., He, Z., and Qiu, X. LongLLaDA: Unlocking Long Context Capabilities in Diffusion LLMs. *arXiv preprint arXiv:2506.14429*, 2025.
- Lou, A., Meng, C., and Ermon, S. Discrete diffusion modeling by estimating the ratios of the data distribution. *arXiv preprint arXiv:2310.16834*, 2023.
- Nie, S., Zhu, F., You, Z., Zhang, X., Ou, J., Hu, J., Zhou, J., Lin, Y., Wen, J.-R., and Li, C. Large language diffusion models. In *Advances in Neural Information Processing Systems (NeurIPS)*, 2025.
- OpenAI. Learning to reason with LLMs. <https://openai.com/index/learning-to-reason-with-llms/>, September 2024.
- Sahoo, S., Arriola, M., Schiff, Y., Gokaslan, A., Marroquin, E., Chiu, J., Rush, A., and Kuleshov, V. Simple and effective masked diffusion language models. *Advances in Neural Information Processing Systems (NeurIPS)*, 2024.
- Sahoo, S. S., Yang, Z., Akhauri, Y., Liu, J., Singh, D., Cheng, Z., Liu, Z., Xing, E., Thickstun, J., and Vahdat, A. Esoteric language models. *arXiv preprint arXiv:2506.01928*, 2025.
- Schulman, J., Wolski, F., Dhariwal, P., Radford, A., and Klimov, O. Proximal policy optimization algorithms. *arXiv preprint arXiv:1707.06347*, 2017.
- Shao, Z., Wang, P., Zhu, Q., Xu, R., Song, J., Bi, X., Zhang, H., Zhang, M., Li, Y., Wu, Y., et al. Deepseekmath: Pushing the limits of mathematical reasoning in open language models. *arXiv preprint arXiv:2402.03300*, 2024.
- Shi, J., Han, K., Wang, Z., Doucet, A., and Titsias, M. Simplified and generalized masked diffusion for discrete data. *Advances in Neural Information Processing Systems (NeurIPS)*, 2024.

- Song, Y., Zhang, Z., Luo, C., Gao, P., Xia, F., Luo, H., Li, Z., Yang, Y., Yu, H., Qu, X., et al. Seed diffusion: A large-scale diffusion language model with high-speed inference. *arXiv preprint arXiv:2508.02193*, 2025.
- Tang, X., Dolga, R., Yoon, S., and Bogunovic, I. wd1: Weighted policy optimization for reasoning in diffusion language models. *arXiv preprint arXiv:2507.08838*, 2025.
- Uehara, M., Zhao, Y., Black, K., Hajiramezanali, E., Scalia, G., Diamant, N. L., Tseng, A. M., Biancalani, T., and Levine, S. Fine-tuning of continuous-time diffusion models as entropy-regularized control. *arXiv preprint arXiv:2402.15194*, 2024.
- Wallace, B., Dang, M., Rafailov, R., Zhou, L., Lou, A., Purushwalkam, S., Ermon, S., Xiong, C., Joty, S., and Naik, N. Diffusion model alignment using direct preference optimization. In *Proceedings of the IEEE/CVF Conference on Computer Vision and Pattern Recognition (CVPR)*, 2024.
- Wang, C., Rashidinejad, P., Su, D., Jiang, S., Wang, S., Zhao, S., Zhou, C., Shen, S. Z., Chen, F., Jaakkola, T., et al. SPG: Sandwiched policy gradient for masked diffusion language models. *arXiv preprint arXiv:2510.09541*, 2025a.
- Wang, G., Schiff, Y., Sahoo, S. S., and Kuleshov, V. Re-masking discrete diffusion models with inference-time scaling. In *Advances in Neural Information Processing Systems (NeurIPS)*, 2025b.
- Wang, G., Schiff, Y., Turok, G., and Kuleshov, V. d2: Improved techniques for training reasoning diffusion language models. *arXiv preprint arXiv:2509.21474*, 2025c.
- Wang, Y., Yang, L., Li, B., Tian, Y., Shen, K., and Wang, M. Revolutionizing reinforcement learning framework for diffusion large language models. *arXiv preprint arXiv:2509.06949*, 2025d.
- Wu, C., Zhang, H., Xue, S., Liu, Z., Diao, S., Zhu, L., Luo, P., Han, S., and Xie, E. Fast-dllm: Training-free acceleration of diffusion LLM by enabling kv cache and parallel decoding. *arXiv preprint arXiv:2505.22618*, 2025.
- Yang, K., Tao, J., Lyu, J., Ge, C., Chen, J., Shen, W., Zhu, X., and Li, X. Using human feedback to fine-tune diffusion models without any reward model. In *Proceedings of the IEEE/CVF Conference on Computer Vision and Pattern Recognition (CVPR)*, 2024.
- Yang, L., Tian, Y., Li, B., Zhang, X., Shen, K., Tong, Y., and Wang, M. Mmada: Multimodal large diffusion language models. *arXiv preprint arXiv:2505.15809*, 2025.
- Ye, J., Gao, J., Gong, S., Zheng, L., Jiang, X., Li, Z., and Kong, L. Beyond autoregression: Discrete diffusion for complex reasoning and planning. *arXiv preprint arXiv:2410.14157*, 2024.
- Ye, J., Xie, Z., Zheng, L., Gao, J., Wu, Z., Jiang, X., Li, Z., and Kong, L. Dream 7B: Diffusion large language models. *arXiv preprint arXiv:2508.15487*, 2025.
- Zhang, K., Zuo, Y., He, B., Sun, Y., Liu, R., Jiang, C., Fan, Y., Tian, K., Jia, G., Li, P., et al. A survey of reinforcement learning for large reasoning models. *arXiv preprint arXiv:2509.08827*, 2025.
- Zhao, H., Liang, D., Tang, W., Yao, D., and Kallus, N. DiFFPO: Training diffusion llms to reason fast and furious via reinforcement learning. *arXiv preprint arXiv:2510.02212*, 2025a.
- Zhao, L., Ding, X., Yu, L., and Akoglu, L. Improving and unifying discrete & continuous-time discrete denoising diffusion. *CoRR*, 2024.
- Zhao, S., Gupta, D., Zheng, Q., and Grover, A. d1: Scaling reasoning in diffusion large language models via reinforcement learning. In *Advances in Neural Information Processing Systems (NeurIPS)*, 2025b.

## A. Theoretical Results

**Theorem 4** (Policy Gradient Theorem). *For a policy  $\pi_\theta$  and the objective  $J(\theta) = \mathbb{E}_{\mathbf{q}, \mathbf{x} \sim \pi_\theta(\cdot | \mathbf{q})} [r(\mathbf{x}_0, \mathbf{q})]$ , the policy gradient is given by (9).*

*Proof.* Writing  $\mathbf{x} = \mathbf{x}_{0:T-1}$ , we can evaluate directly

$$\begin{aligned} \nabla_\theta J(\theta) &= \nabla_\theta \mathbb{E}_{\mathbf{q}} \left[ \sum_{\mathbf{x}} r(\mathbf{x}_0, \mathbf{q}) \pi_\theta(\mathbf{x} | \mathbf{q}) \right] = \mathbb{E}_{\mathbf{q}} \left[ \sum_{\mathbf{x}} r(\mathbf{x}_0, \mathbf{q}) \nabla_\theta \pi_\theta(\mathbf{x} | \mathbf{q}) \right] \\ &= \mathbb{E}_{\mathbf{q}} \left[ \sum_{\mathbf{x}} r(\mathbf{x}_0, \mathbf{q}) \pi_\theta(\mathbf{x} | \mathbf{q}) \nabla_\theta \log \pi_\theta(\mathbf{x} | \mathbf{q}) \right] = \mathbb{E}_{\mathbf{q}, \mathbf{x} \sim \pi_\theta(\cdot | \mathbf{q})} [r(\mathbf{x}_0, \mathbf{q}) \nabla_\theta \log \pi_\theta(\mathbf{x} | \mathbf{q})]. \end{aligned}$$

By definition, since  $\pi_\theta(\mathbf{x} | \mathbf{q}) = \pi_\theta(\mathbf{x}_{0:T-1} | \mathbf{q}) = \prod_{t=0}^{T-1} \pi_\theta(\mathbf{x}_t | \mathbf{x}_{t+1}, \mathbf{q})$ , we have  $\nabla_\theta J(\theta) = \sum_{t=0}^{T-1} \nabla_\theta J_t(\theta)$ , where the per step policy gradient is defined as  $\nabla_\theta J_t(\theta) = \mathbb{E}_{\mathbf{q}, \mathbf{x} \sim \pi_\theta} [r(\mathbf{x}_0, \mathbf{q}) \nabla_\theta \log \pi_\theta(\mathbf{x}_t | \mathbf{x}_{t+1}, \mathbf{q})]$ . The term inside the expectation is a random variable that depends on  $\mathbf{x}_t, \mathbf{x}_{t+1}, \mathbf{x}_0, \mathbf{q}$ . For any action  $\mathbf{x}_t$  independent baseline, in particular, the random variable  $V_{t+1}^{\pi_\theta}(\mathbf{x}_{t+1})$ , we have

$$\begin{aligned} &\mathbb{E}_{\mathbf{x}_t \sim \pi_\theta(\cdot | \mathbf{x}_{t+1})} [V_{t+1}^{\pi_\theta}(\mathbf{x}_{t+1}) \nabla_\theta \log \pi_\theta(\mathbf{x}_t | \mathbf{x}_{t+1})] = V_{t+1}^{\pi_\theta}(\mathbf{x}_{t+1}) \mathbb{E}_{\mathbf{x}_t \sim \pi_\theta(\cdot | \mathbf{x}_{t+1})} [\nabla_\theta \log \pi_\theta(\mathbf{x}_t | \mathbf{x}_{t+1})] \\ &= V_{t+1}^{\pi_\theta}(\mathbf{x}_{t+1}) \sum_{\mathbf{x}_t} \pi_\theta(\mathbf{x}_t | \mathbf{x}_{t+1}) \nabla_\theta \log \pi_\theta(\mathbf{x}_t | \mathbf{x}_{t+1}) = V_{t+1}^{\pi_\theta}(\mathbf{x}_{t+1}) \sum_{\mathbf{x}_t} \nabla_\theta \pi_\theta(\mathbf{x}_t | \mathbf{x}_{t+1}) \\ &= V_{t+1}^{\pi_\theta}(\mathbf{x}_{t+1}) \nabla_\theta \left( \sum_{\mathbf{x}_t} \pi_\theta(\mathbf{x}_t | \mathbf{x}_{t+1}) \right) = V_{t+1}^{\pi_\theta}(\mathbf{x}_{t+1}) \nabla_\theta(1) = 0. \end{aligned}$$

Therefore,  $A_t^{\pi_\theta} = r(\mathbf{x}_0, \mathbf{q}) - V_{t+1}^{\pi_\theta}(\mathbf{x}_{t+1}, \mathbf{q})$  satisfies  $\nabla_\theta J_t(\theta) = \mathbb{E}_{\mathbf{q}, \mathbf{x} \sim \pi_\theta(\cdot | \mathbf{q})} [A_t^{\pi_\theta} \nabla_\theta \log \pi_\theta(\mathbf{x}_t | \mathbf{x}_{t+1})]$ .  $\square$

**Proposition 5** (Entropy Bound). *Let  $\pi_\theta$  be a softmax policy with logits  $g_\theta^i$  for  $i$  over a finite set, i.e.,  $\pi_{\theta,i} \triangleq \frac{\exp(g_{\theta,i})}{\sum_{i'} \exp(g_{\theta,i'})}$ . Let  $A_i$  be constants such that  $\|A\|_\infty \triangleq \max_i |A_i|$  is finite. Let  $J(\theta) \triangleq \mathbb{E}_{i \sim \pi_\theta} [A_i]$  and suppose  $\|\nabla_\theta g_\theta\| \triangleq \max_{i,j} \|\nabla_\theta (g_{\theta,i} - g_{\theta,j})\|$  is bounded. Then,  $\nabla_\theta J(\theta) = \mathbb{E}_{i \sim \pi_\theta} [A_i \nabla_\theta \log \pi_{\theta,i}]$  satisfies*

$$\|\nabla_\theta J(\theta)\| \leq H(\pi_\theta) \|A\|_\infty \|\nabla_\theta g_\theta\|, \quad (21)$$

where  $H(\pi_\theta) \triangleq \mathbb{E}_{i \sim \pi_\theta} [-\log \pi_{\theta,i}]$  is the entropy of  $\pi_\theta$ .

*Proof.* Starting with the gradient of the objective  $J$ , we have  $\|\nabla_\theta J(\theta)\| \leq \mathbb{E}_{i \sim \pi_\theta} [|A_i| \|\nabla_\theta \log \pi_{\theta,i}\|] \leq \|A\|_\infty \mathbb{E}_{i \sim \pi_\theta} [\|\nabla_\theta \log \pi_{\theta,i}\|]$ . Now, for any  $i$ , using chain-rule and the derivative of softmax policy, we have  $\nabla_\theta \log \pi_{\theta,i} = (1 - \pi_{\theta,i}) \nabla_\theta g_{\theta,i} - \sum_{j \neq i} \pi_{\theta,j} \nabla_\theta g_{\theta,j} = \sum_{j \neq i} \pi_{\theta,j} (\nabla_\theta g_{\theta,i} - \nabla_\theta g_{\theta,j})$ . Therefore, by triangle inequality, we obtain

$$\|\nabla_\theta \log \pi_{\theta,i}\| \leq \sum_{j \neq i} \pi_{\theta,j} \|\nabla_\theta (g_{\theta,i} - g_{\theta,j})\| \leq \left( \sum_{j \neq i} \pi_{\theta,j} \right) \left( \max_{i,j} \|\nabla_\theta (g_{\theta,i} - g_{\theta,j})\| \right) \quad (22)$$

$$= (1 - \pi_{\theta,i}) \|\nabla_\theta g_\theta\| \leq (-\log \pi_{\theta,i}) \|\nabla_\theta g_\theta\|, \quad (23)$$

where the last step follows from  $1 - x \leq -\log x$  for  $x \in (0, 1)$ . Using the above bound in the first inequality gives the result.  $\square$

*Proof of Theorem 3.* By Proposition 5, we obtain the following bound on the error in terms of the per-step entropy:

$$\Delta_S = \|\nabla_\theta J(\theta) - \nabla_\theta J_S(\theta)\| = \left\| \sum_{t \notin S} \nabla_\theta J_t(\theta) \right\| \leq \sum_{t \notin S} \|\nabla_\theta J_t(\theta)\| \leq \sum_{t \notin S} H(\pi_\theta^{t|t+1}) \|A_t^{\pi_\theta}\|_\infty \|\nabla_\theta g_\theta^{t|t+1}\|,$$

where  $g_\theta$  are the logits from which the policy  $\pi_\theta$  is constructed by taking softmax. From the assumptions in the lemma, we obtain the bound on the error as  $\Delta_S \leq B \sum_{t \notin S} H(\pi_\theta^{t|t+1})$ .  $\square$

## B. Datasets and Reward Functions

We largely follow the experimental protocol of d1 (Zhao et al., 2025b), adopting the same reward formulations and train–test splits to ensure comparability.

### B.1. GSM8K.

We use the training split of the GSM8K dataset for reinforcement learning and evaluate on the official test split. Rewards follow the Unsloth-style formulation and consist of five additive components:

- an XML structure reward that assigns +0.125 for each correctly placed formatting tag, with small penalties for extraneous content appearing after closing tags;
- a soft format reward of +0.5 for outputs matching the pattern `<reasoning>...</reasoning><answer>...</answer>`
- a strict format reward of +0.5 for exact adherence to the expected structure, including correct line breaks;
- an integer-answer reward of +0.5 if the predicted answer is a valid integer;
- a correctness reward of +2.0 when the predicted answer matches the ground-truth solution.

### B.2. MATH500.

For MATH500, we train on the training split and evaluate on the test split. The reward function consists of formatting and correctness components:

- a format reward of 1.0 if `<answer></answer>` tags are present and the answer is enclosed in a `\boxed` expression;
- a format reward of 0.75 if `<answer></answer>` tags are present without a boxed expression;
- a format reward of 0.5 if a boxed expression is present without answer tags;
- a format reward of 0.25 if neither answer tags nor a boxed expression are present;
- a correctness reward of +2.0 when the boxed answer exactly matches the ground-truth solution.

### B.3. Sudoku.

For the  $4 \times 4$  Sudoku task, we use a publicly available dataset of one million synthetically generated puzzles.<sup>1</sup> The dataset was generated using the Arel solver. For evaluation, we randomly sample 256 puzzles using the same generator. The reward is computed as the fraction of correctly filled cells among positions that were initially empty in the input puzzle, focusing evaluation on reasoning performance rather than copying pre-filled values.

### B.4. Coding.

For coding experiments, we train on the KodCode-Light-RL-10k dataset. The reward function consists of three components. First, an XML structure reward identical to GSM8K is used, with an additional +0.5 bonus when the generated program is enclosed within answer tags; outputs not wrapped in `python` code blocks receive zero structural reward. Second, a correctness score is computed using unit tests, where the reward corresponds to the fraction of tests passed rather than a binary success signal. Finally, a safety constraint assigns a reward of 0 if the generated code imports restricted modules, including `os`, `sys`, `shutil`, `subprocess`, `socket`, `psutil`, `ctypes`, `pathlib`, `builtins`, or `import`.

---

<sup>1</sup><https://github.com/Black-Phoenix/4x4-Sudoku-Dataset>

---

**Algorithm 1** Entropy-Guided Stepwise Policy Optimization with Stepwise Advantages (EGSPO-SA)
 

---

**Require:** Policy  $\pi_\theta$ , reference policy  $\pi_{\text{ref}}$ , reward  $r$ , prompt distribution  $\mathcal{D}$ , denoising steps  $T$ , step budget  $K$ , completions  $G$ , advantage weight  $\lambda$ , KL weight  $\beta$

- 1: Initialize  $\theta \leftarrow \theta_{\text{ref}}$
  - 2: **while** not converged **do**
  - 3:   Sample prompt  $\mathbf{q} \sim \mathcal{D}$
  - 4:   Sample  $G$  diffusion trajectories  $\mathbf{x}_{0:T}^j \sim \pi_{\theta_{\text{old}}}(\cdot | \mathbf{q})$  for  $j = 1, \dots, G$
  - 5:   Compute  $\pi_{\text{ref}}(\mathbf{x}_t^j | \mathbf{x}_{t+1}^j)$  for  $j = 1, \dots, G, t = 0, \dots, T - 1$
  - 6:   Compute per-step entropies  $H_t^j$  of  $\pi_{\theta_{\text{old}}}(\cdot | \mathbf{x}_{t+1}^j)$
  - 7:   Select step subset  $S^j \leftarrow \text{top}[K](t : H_t^j)$
  - 8:   Greedly complete trajectory from  $\mathbf{x}_{t+1}^j$ :  $\hat{\mathbf{x}}_{0|t+1}^j \leftarrow \text{GreedyComplete}(\mathbf{x}_{t+1}^j)$  (as per Eq. (20))
  - 9:   Estimate step advantages per completion:  $A_t^j \leftarrow (1 + \lambda)r(\mathbf{x}_0^{(j)}, \mathbf{q}) - \lambda r(\hat{\mathbf{x}}_{0|t+1}^j, \mathbf{q})$ .
  - 10:   Compute centered stepwise advantages:  $\bar{A}_t^j \leftarrow A_t^j - \frac{1}{G} \sum_{i=1}^G A_t^i$
  - 11:   Compute importance ratios  $\rho_t^j \leftarrow \pi_\theta(\mathbf{x}_t^j | \mathbf{x}_{t+1}^j) / \pi_{\theta_{\text{old}}}(\mathbf{x}_t^j | \mathbf{x}_{t+1}^j)$
  - 12:   Estimate KL term using  $\pi_\theta$  and  $\pi_{\text{ref}}$  likelihoods using trajectories from  $\pi_{\theta_{\text{old}}}$
  - 13:   Update  $\pi_\theta$  using GRPO with stepwise advantages  $\bar{A}_t^j$  and KL regularization weighted by  $\beta$
  - 14: **end while**
  - 15: Return  $\pi_\theta$
- 

### C. Hyperparameter Settings and Implementation Details

We follow prior diffusion-RL work for most hyperparameter choices. Low-Rank Adaptation (LoRA) is applied with rank  $r = 128$  and scaling factor  $\alpha = 64$ . Training is conducted on 8 NVIDIA A100 GPUs. We use a batch size of 6 prompts per GPU with a gradient accumulation step of 2, resulting in an effective batch size of 96 prompts per update. Optimization is performed using Adam with  $\beta_1 = 0.9$ ,  $\beta_2 = 0.99$ , weight decay of 0.1, and a learning rate of  $3 \times 10^{-5}$ .

For RL rollout, we use a generation length of 256 tokens with 128 denoising steps during training. We adopt block-wise generation with a block size of 32, and two tokens are denoised in parallel at each step for all tasks. For each prompt, we generate 8 completions, and for each completion, we select the top  $K = 8$  denoising steps with the highest entropy for policy updates. We use a temperature of 0.9 during training for all tasks except Countdown, where a temperature of 0.2 is used. At inference time, we apply greedy decoding for all tasks.

At evaluation time, we report results using generation lengths of 128, 256, and 512 tokens. Models are evaluated once the reward curves stabilize. Coding tasks are trained for 4k steps, mathematical reasoning tasks for around 6k steps, and logical reasoning tasks for 10k steps. For all tasks, we select the checkpoint with the highest average performance across the evaluated generation lengths. For logical reasoning tasks and GSM8K, we use a static  $\lambda = 1$  for all time steps. For Math benchmark and coding tasks, we use a dynamic  $\lambda$  schedule, initialized at 1 and halved every 500 steps.

### D. Algorithms

Algorithm 1 summarizes the proposed entropy-guided reinforcement learning procedure for diffusion language models. EGSPO-SA operates directly on the denoising process by treating each denoising step as an action and optimizing the policy using a GRPO-style objective.

The method applies entropy-based step selection to identify a subset of informative denoising timesteps for policy updates, avoiding unnecessary optimization at low-entropy, near-deterministic steps. In addition, EGSPO-SA incorporates stepwise advantages based on intermediate reward-to-go estimates. For each selected denoising step, the partial trajectory is greedily completed to estimate the remaining reward, which is used as a baseline for credit assignment. This yields denser and more precise training signals along the denoising trajectory.

EGSPO corresponds to a special case of EGSPO-SA obtained by setting the advantage weight  $\lambda = 0$ , in which a single sequence-level reward is broadcast uniformly across the selected denoising steps.

## E. Qualitative Examples on Sudoku

We provide qualitative examples comparing the EGSPPO and EGSPPO-SA with d1 on representative tasks to illustrate differences in reasoning behavior and outputs.

**Sudoku Example**

**Problem.** Solve the following  $4 \times 4$  Sudoku puzzle:

0000304014022304

**Ground Truth.**

4123324114322314

**Model Generations.**

- **EGSPPO-SA (Correct)**

To solve this Sudoku puzzle, we need to fill the empty cells with the digits 1-4 such that each row, each, and each  $2 \times 2$  box contains all the digits exactly once. We can start by filling the first row with the digits 3 and 4. Then, we can fill the second row with the digits 1 and 4. Next, we can fill the remaining rows and columns with the remaining digits. </reasoning> <answer> 4123324114322314 </answer>
- **EGSPPO (Correct)**

To solve the  $4 \times 4$  Sudoku puzzle, we need to fill in the empty cells with the digits 1-4 such that each row, column, and  $2 \times 2$  box contains the digits 1-4 exactly once. We can start by analyzing the given puzzle and filling in the empty cells according to the rules. We need to ensure that each row, column, and  $2 \times 2$  box contains the digits 1-4 exactly once. </reasoning> <answer> 4123324114322314 </answer>
- **d1 (Incorrect)**

To solve this  $4 \times 4$  Sudoku puzzle, we need to fill in the empty cells with digits 1-4 such that each row, column, and  $2 \times 2$  box contains all digits exactly once. We can start by placing the known digits and then filling in the empty cells guided by the rules of Sudoku. We will use a systematic approach to fill in the grid, ensuring that each row, column, and box conforms to the Sudoku rules. </reasoning> <answer> 1234314214322314 </answer>

**Sudoku Example**

**Problem.** Solve the following  $4 \times 4$  Sudoku puzzle:

0400010002311340

**Ground Truth.**

2413312442311342

**Model Generations.**

- **EGSPPO-SA (Correct)**

To solve this Sudoku puzzle, we need to fill the empty cells with the digits 1-4 such that each row, each, and each  $2 \times 2$  box contains all the digits exactly once. We can start by filling the first row with the digits 4 and 1. Then, we can fill the second row with the digits 3 and 3. Next, we can fill the remaining rows and columns with the remaining digits. </reasoning> <answer> 2413312442311342 </answer>
- **EGSPPO (Correct)**

To solve the  $4 \times 4$  Sudoku puzzle, we need to fill in the empty cells with the digits 1-4 such that each row, column, and  $2 \times 2$  box contains the digits 1-4 exactly once. We can start by analyzing the given puzzle and filling in the empty cells according to the rules. We need to ensure that each row, column, and  $2 \times 2$  box contains the digits 1-4 exactly once. </reasoning> <answer> 2413312442311342 </answer>
- **d1 (Incorrect)**

To solve this  $4 \times 4$  Sudoku puzzle, we need to fill in the empty cells with digits 1-4 such that each row, column, and  $2 \times 2$  box contains all digits exactly once. We can start by placing the known digits and then use logical deduction to fill in the remaining cells. We will use the process of and process of elimination to solve the puzzle. . . . . </reasoning> <answer> 1234412323413412 </answer>

## **F. LLM Usage**

Large language models were used solely as an editorial aid to improve clarity and presentation. No scientific content, including methods, algorithms, formulas, experimental design, or results, was generated or suggested by LLMs. All technical contributions and conclusions are the original work of the authors.